Global metabolic responses of mice to *Trypanosoma brucei brucei* infection

Yulan Wang*†, Jürg Utzinger‡, Jasmina Saric*‡, Jia V. Li*‡, Jean Burckhardt§, Stephan Dirnhofer¶, Jeremy K. Nicholson*, Burton H. Singer||**, Reto Brun††, and Elaine Holmes*,**

*Department of Biomolecular Medicine, Division of Surgery, Oncology, Reproductive Biology and Anaesthetics, Faculty of Medicine, Imperial College London, London SW7 2AZ, United Kingdom; Departments of ‡Public Health and Epidemiology and ††Medical Parasitology and Infection Biology, Swiss Tropical Institute, CH-4002 Basel, Switzerland; §Department of Biomedicine/Endocrinology and ¶Institute of Pathology, University Hospital Basel, CH-4031 Basel, Switzerland; and ||Office of Population Research, Princeton University, Princeton, NJ 08544

Contributed by Burton H. Singer, February 25, 2008 (sent for review November 9, 2007)

Human African trypanosomiasis (HAT) is transmitted by tsetse flies and, if untreated, is fatal. Treatment depends on infection stage, and early diagnosis is crucial for effective disease management. The systemic host biochemical changes induced by HAT that enable biomarker discovery or relate to therapeutic outcome are largely unknown. We have characterized the multivariate temporal responses of mice to *Trypanosoma brucei brucei* infection, using ^{1}H nuclear magnetic resonance (NMR) spectroscopic metabolic phenotyping of urine and plasma. Marked alterations in plasma metabolic profiles were detected already 1 day postinfection. Elevated plasma concentrations of lactate, branched chain amino acids, and acetylglycoprotein fragments were noted. *T. brucei brucei*-infected mice also had an imbalance of plasma alanine and valine, consistent with differential gluconeogenesis (parasite)-ketogenesis (host) pathway counterflux, involving stimulated host glycolysis, ketogenesis, and enhanced lipid oxidation in the host. Histopathologic evidence of *T. brucei brucei*-induced extramedullary hepatic hemopoiesis, renal interstitial nephritis, and a provoked inflammatory response was also noted. Metabolic disturbance of gut microbiotal activity was associated with infection, as indicated by changes in the urinary concentrations of the microbial co-metabolites, including hippurate. Concluding, parasite infection results in multiple systemic biochemical effects in the host and disturbance of the symbiotic gut microbial metabolic interactions. Investigation of these transgenomic metabolic alterations may underpin the development of new diagnostic criteria and metrics of therapeutic efficacy.

diagnosis | metabonomics | NMR spectroscopy | trypanosomiasis

Human African trypanosomiasis (HAT), also known as sleeping sickness, is a so-called neglected tropical disease (1). It is caused by two subspecies of the protozoan parasite *Trypanosoma brucei*: *Trypanosoma brucei gambiense* occurs in western and central Africa, and *Trypanosoma brucei rhodesiense* is endemic in the eastern and southern parts of Africa (2, 3). The route of transmission is through the bite of infected tsetse flies (3). *T. brucei brucei* represents the third subspecies; it is not infectious to humans but can cause disease in cattle, goats, and sheep (i.e., nagana), and therefore contributes to the societal impact of these diseases. In the 1980s and 1990s, there was a major reemergence of HAT, due to war, migration, environmental deterioration, increasing parasite drug resistance, and lack of surveillance (4, 5). It is currently estimated that 60 million people are at risk of HAT, with an average annual incidence of 30,000 cases (2).

The infection evolves in two stages: first the hemolymphatic stage (usually occurring 1–3 weeks after the bite of an infectious tsetse fly), followed by the meningo-encephalitic stage. During the hemolymphatic stage, trypanosomes enter the bloodstream and cause nonspecific symptoms, including malaise, headache, weakness, and joint pain. The meningo-encephalitic stage is marked once trypanosomes have crossed the blood–brain barrier, and therefore penetrate the central nervous system (CNS). The onset is insidious and evokes a wide clinical phenotype, causing an array of neurological disorders, including motor, psychiatric, and sensory abnormalities, and disturbed sleep cycles, thus the term "sleeping sickness." An infection eventually leads to seizures, coma, and death if untreated. Treatment is tailored to the stages of the disease, but is generally unsatisfactory.

There is a need to adopt effective diagnosis, which is able to give not only clear indication of trypanosome infection, but also an accurate staging of HAT, because failure to treat patients with CNS involvement will ultimately always lead to death. The current lack of early diagnostic tools and the absence of safe and efficacious drugs remain major bottlenecks for sound disease surveillance and control (3, 6, 7). Specific diagnosis at the early stage of disease involves the demonstration of the parasite in the peripheral blood or lymph node aspirates, which is, however, unreliable at low parasitemia. Serological tests play an important role: e.g., antibody-detecting card agglutination trypanosomiasis test (CATT) and latex agglutination test (LATEX/Tbg) (8, 9). Identification of disease stage invariably involves a lumbar puncture, which is invasive and thus unsuitable for large-scale screening purpose (10).

Clinical manifestations of HAT are nonspecific (4); therefore, there is an unmet need for a reproducible biomarker or surrogate marker for disease presence and stage of infection. To be useful in the diagnosis of this disease, such a biomarker must be robust, exhibit high sensitivity and selectivity, and change with disease stage. With the advent of "omics" technologies, new approaches to the diagnosis of infectious diseases have been made possible. Both genomic and proteomic approaches have been applied to the diagnosis of HAT (11, 12). However, as yet no satisfactory biomarkers, or combination thereof, have been identified.

Metabonomics offers an alternative approach to characterizing biomarkers of disease in accessible biological samples such as urine and blood plasma. This approach typically employs high-resolution spectroscopic methods, such as ^{1}H nuclear magnetic resonance (NMR) spectroscopy or mass spectrometry (MS) to provide a fingerprint of biological samples. These fingerprints can be interpreted and classified according to disease status by using multivariate statistical analysis (13). Although metabonomics has been successfully used in many fields, e.g., in the study of disease processes (14, 15) and dietary intervention (16, 17), the application

Author contributions: Y.W., J.U., J.B., J.K.N., B.H.S., R.B., and E.H. designed research; Y.W., J.U., J.S., J.V.L., J.B., S.D., and R.B. performed research; Y.W., J.S., J.V.L., S.D., and E.H. analyzed data; and Y.W., J.U., J.K.N., B.H.S., and E.H. wrote the paper.

The authors declare no conflict of interest.

†Present address: State Key Laboratory of Magnetic Resonance and Atomic and Molecular Physics, Wuhan Institute of Physics and Mathematics, Chinese Academy of Sciences, Wuhan 430071, China.

**To whom correspondence may be addressed. E-mail: elaine.holmes@imperial.ac.uk or singer@princeton.edu.

This article contains supporting information online at www.pnas.org/cgi/content/full/0801777105/DCSupplemental.

of this technology to characterize parasitic diseases is still in its infancy.

Previous studies of metabolic changes in response to *Schistosoma mansoni* and *Schistosoma japonicum* infection in rodent models indicated that a characteristic metabolic fingerprint could be derived for each type of infection (14, 18). In the current study, we evaluated the time course of systemic metabolic effects of *T. brucei brucei* exposure in mice. Our objective is to use NMR spectroscopy as an exploratory tool to determine a metabolic signature of the different stages of *T. brucei brucei* infection to further our understanding of host-parasite interactions, which could then lead to the development of biochemical assays. The ultimate aim is to provide the basis for accurate diagnosis and staging of HAT and come forward with new metrics for measuring the efficacy of interventional therapeutics.

Results

Experimental Setup and Rationale. To establish metabolic changes associated with *T. brucei brucei* infection, urine and plasma were collected from 12 mice 2 days before infection and at a series of time points over a 33-day study period postinfection. Urine and plasma were also collected from 12 uninfected mice that served as control.

In addition, a satellite group of mice (n = 48) was used to establish the time at which the parasites crossed the blood–brain barrier. For the GVR35 strain of *T. brucei brucei* in the mouse model, it has been reported that at day 21 postinfection parasites have established in the brain (4). However, because parasite strains maintained under laboratory conditions can alter in virulence (19), it was important to ascertain at which time point trypanosomes had crossed the blood–brain barrier in our model [for details, see supporting information (SI) *Text*]. The results indicated that *T. brucei brucei* established in the brain within 7 days.

Parasitemia, Bodyweight, and Histology. No change in the body weight of the infected mice occurred and parasitemia levels were consistent with the literature (*SI Text*). On termination, control mice showed no abnormalities in cellular architecture in either the liver or kidney. All infected animals manifested marked hepatic extramedullary hemopoiesis and renal interstitial nephritis (Fig. S1).

^{1}H NMR Spectra of Urine and Plasma. ^{1}H NMR spectra of urine obtained from a mouse at three time points, i.e., preinfection, and days 14 and 28 postinfection, are plotted in Fig. 1. Preinfection urine spectra were consistent with previously reported metabolite profiles for this murine strain (14). Changes in the urinary profiles were observed in *T. brucei brucei*-infected mice when compared with the samples taken from the same mice at preinfection stage: e.g., increase in concentrations of lactate, 2-oxoisocaproate, 2-oxoisovalerate, D-3-hydroxybutyrate, and taurine. Additionally, three singlets not reported previously at δ 1.66, δ 1.70, and δ 1.71 (Fig. 1) were observed in 23 of the 24 mice and were assigned as 3-methylcrotonic acid, which disappeared or was reduced in the urine from both infected and control mice at later time points. Because these resonances are not always present in urine spectra from mice of the same strain, they are unreliable as markers of a general *T. brucei brucei* infection. A doublet at δ 1.08 (Fig. 1), which appeared only in the infected mice, was directly linked with a resonance at δ 2.50 in the ^{1}H-^{1}H correlation spectroscopy (COSY) spectrum, and with δ 3.18, δ 3.55, and δ 3.72 in the total correlation spectroscopy (TOCSY) spectrum, and was tentatively assigned as 3-carboxy-2-methyl-3-oxopropanamine.

Examples of ^{1}H standard 1-dimensional (1D) NMR spectra of plasma obtained from a representative mouse, i.e., preinfection, days 14 and 28 postinfection, are presented in Fig. 2. Several differences between the preinfection and postinfection states could be observed. For example, reduced amino acid levels were noted in plasma of *T. brucei brucei*-infected mice. To generate an overview

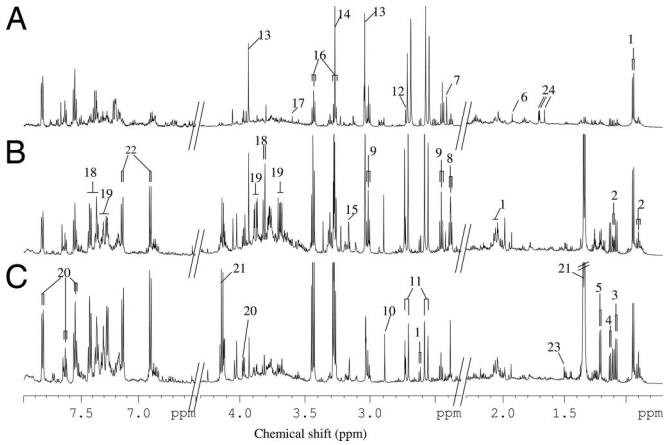

Fig. 1. Typical 600 MHz ^{1}H NMR spectra of urine obtained from a mouse at preinfection (*A*), at 14 days postinfection (*B*), and at 28 days postinfection (*C*). The spectra in the aromatic region (δ 6.5–8.0) were magnified 4 times compared with the region δ 2.3–4.3, whereas the region δ 0.7–2.3 was magnified twice. Key: 1, 2-oxoisocaproate; 2, 3-methyl-2-oxovalerate; 3, 3-carboxy-2-methyl-3-oxopropanamine; 4, 2-oxoisovalerate; 5, D-3-hydroxybutyrate; 6, acetate; 7, succinate; 8, β-alanine; 9, 2-oxoglutarate; 10, trimethylamine; 11, citrate; 12, dimethylamine; 13, creatine; 14, trimethylamine-*N*-oxide; 15, malonate; 16, taurine; 17, glycine; 18, phenylacetylglycine; 19, tryptophan; 20, hippurate; 21, lactate; 22, 4-hydroxyphenylacetic acid; 23, alanine, 24, methylcrotonic acid.

of metabolite patterns and to identify biomarkers of the temporal biological response to a *T. brucei brucei* infection, multivariate data analysis of ^{1}H NMR profiles of urine and plasma from the 12 infected mice was carried out over the seven collection times spanning the study duration.

Disease Progression. To characterize the evolution of the disease with time, principal component analysis (PCA) was performed on the ^{1}H NMR spectral data of the urine and plasma from all of the time points using mean centered data. For the plasma samples, the scores plots showed differentiation of the preinfection samples from all other time points with greater separation and dispersion between animals at the later time points (Fig. 3*A*). Clear separation of all early (days 1–14) postinfection plasma samples from preinfection samples was established in a further PCA model (Fig. 3*E*). The scores of the first and second principal components (PCs) were averaged for the group of infected mice at each time point and plotted in Fig. 3*B*. The trajectory indicated that the infected mice

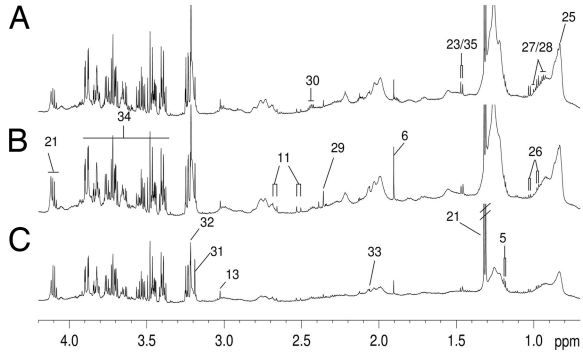

Fig. 2. Representative 600 MHz ^{1}H NMR spectra of plasma using a standard 1D water presaturation pulse sequence from a mouse at preinfection (*A*), at 14 days postinfection (*B*), and at 28 days postinfection (*C*). Key: 5, D-3-hydroxybutyrate; 6, acetate; 11, citrate; 13, creatine; 21, lactate; 23, alanine; 25, lipoprotein; 26, valine; 27/28, leucine and isoleucine; 29, oxaloacetate; 30, glutamine; 31, choline; 32, phosphatidylcholine; 33, *O*-acetyl-glycoprotein fragments; 34, glucose; 35, lysine.

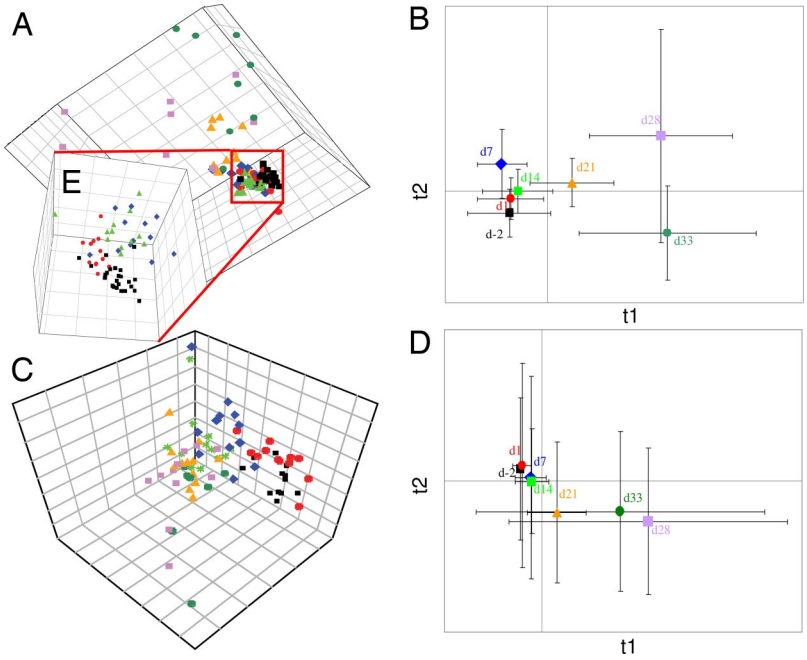

Fig. 3. Pseudo three-dimensional (3D) score plots obtained from the PCA of ^{1}H NMR spectra of plasma (*A*), and urine (*C*); *B* and *D* are the trajectory of PCA score plots of PC1 (t[1]) versus PC2 (t[2]) for ^{1}H NMR spectra of plasma and urine, respectively, obtained at different time points with error bars representing two standard deviations. Black (d−2), preinfection. Red (d1), blue (d7), green (d14), yellow (d21), pink (d28), and dark green (d33) denote samples collected at day 1, 7, 14, 21, 28, and 33 postinfection, respectively. (*E*) 3D score plots obtained from the PCA of ^{1}H NMR spectra of plasma obtained from d−2, d1, d7, and d14 showing clear differentation of preinfection and infection at early time points, which are otherwise obscured by the extreme variation in metabolite profiles observed at later time points.

deviated from the controls along the PC2 direction after *T. brucei brucei* inoculation up to day 14 and subsequently moved in the PC1 direction. In addition, 21 days postinfection, the samples were more dispersed in metabolic space compared with the samples obtained from days 1–14 postinfection, as demonstrated by the standard deviation bars (Fig. 3*B*).

For the urine samples the scores plots showed a similar time-related behavior to those calculated for the plasma (Fig. 3 *C* and *D*). To eliminate the contribution of growth and maturation in the mice to the differentiation of later time points from the preinfection samples, the same PCA strategy was applied to the ^{1}H NMR data obtained from the control mice. No significant time-related movement of the metabolic profiles was found. An orthogonal signal correction-partial least square-discriminant analysis (O-PLS-DA), performed on spectra obtained from each time point postinfection (i.e., days 1, 7, 14, 21, 28, and 33) in pairwise comparison with those obtained from the preinfection control mice, showed systematic metabolic changes for both urine and plasma.

Characterization of Sequential Urinary Metabolic Changes Associated with *T. brucei brucei* Infection. Potential urinary biomarkers of a trypanosome infection and stage were identified by using an O-PLS-DA method. One PLS component was calculated for each model by using unit variance scaled data with one orthogonal component to remove the variables in NMR spectra unrelated to the variation between the two classes. The total explained variation for the *X*-matrix (NMR data) was indicated by the R^2 value (0.88–0.91 for all time points except day 1 postinfection; Table 1) and the corresponding cross-validation parameter indicating the predictive performance of the model (Q^2) reflected a high predictive ability (i.e., >0.73 for all time points except day 1 postinfection; Table 1). Model outcomes indicated that the metabolic differentiation between the preinfection and postinfection time points was highly significant from day 7 onwards.

Interpretation of the differences between the ^{1}H NMR spectra of urine from mice before and after infection was carried out by using O-PLS-DA cross-validated coefficient plots with results shown in Fig. S2*A*. Key metabolites contributing to the separation of preinfection data from the postinfection data, along with their significance values, are summarized in Table 1. A coefficient >0.53 is considered to be significant as this coefficient corresponds to the critical value of a correlation coefficient with a risk of 5%.

The urine samples obtained at day 7 postinfection deviated from the corresponding controls because of the increased urinary excretion of 3-methyl-2-oxovalerate, trimethylamine, tryptophan, and 4-hydroxyphenyl acetic acid in the infected mice. These changes were associated with decreased urinary excretion of 3-methylcrotonic acid, creatine, and hippurate in the infected

Table 1. Metabolite changes in mouse urine induced by *T. brucei brucei* infection

Metabolites*	δ, ppm	Day 1 R^2 = 0.06 Q^2 = 0.78	Day 7 R^2 = 0.88 Q^2 = 0.73	Day 14 R^2 = 0.94 Q^2 = 0.87	Day 21 R^2 = 0.94 Q^2 = 0.87	Day 28 R^2 = 0.90 Q^2 = 0.86	Day 33 R^2 = 0.91 Q^2 = 0.78
3-Carboxy-2-methyl-3-oxopropanamine (3)	1.08	—	—	+0.71	+0.75	+0.87	+0.81
3-Methyl-2-oxovalerate (2)	1.11	—	+0.50	+0.72	+0.84	+0.74	+0.77
2-Oxoisovalerate (4)	1.14	—	—	+0.59	+0.69	—	—
D-3-hydroxybutyrate (5)	1.20	—	—	—	+0.74	+0.75	+0.75
Lactate (21)	1.33	—	—	—	+0.66	+0.65	+0.68
Methylcrotonic acid (24)	1.70	—	−0.57	−0.48	−0.54	−0.63	—
Trimethylamine (10)	2.89	—	+0.49	+0.62	+0.51	+0.51	—
Tryptophan (19)	7.30	—	+0.64	+0.78	+0.78	+0.84	+0.74
4-Hydroxyphenylacetic acid (22)	7.14	—	+0.64	+0.73	+0.73	+0.72	+0.82
Hippurate (20)	7.83	—	−0.66	−0.59	−0.71	−0.70	−0.66

*Numbers in parentheses refer to metabolites shown in Fig. 1, Fig. 2, and Fig. S2.

Table 2. Metabolite changes in mouse plasma induced by *T. brucei brucei* infection

Metabolites*	δ, ppm	Day 1 $R^2 = 0.90$ $Q^2 = 0.61$	Day 7 $R^2 = 0.94$ $Q^2 = 0.72$	Day 14 $R^2 = 0.95$ $Q^2 = 0.75$	Day 21 $R^2 = 0.96$ $Q^2 = 0.82$	Day 28 $R^2 = 0.96$ $Q^2 = 0.74$	Day 33 $R^2 = 0.94$ $Q^2 = 0.61$
Lactate (21)	1.33	+0.65	+0.76	+0.83	+0.76	+0.74	+0.77
Glutamine (30)	2.30	−0.50	−0.80	−0.72	—	—	—
Oxaloacetate (29)	2.36	+0.69	+0.66	—	+0.51	+0.51	+0.66
Lysine (35)	1.45	—	—	—	+0.62	+0.79	+0.82
Glucose (34)	5.23	+0.56	—	—	—	−0.58	−0.59
Isoleucine (28)	0.95	—	−0.86	−0.82	−0.88	−0.83	−0.78
Valine (26)	0.98	—	−0.81	−0.76	−0.81	−0.80	−0.83
Leucine (27)	1.00	—	−0.88	−0.84	−0.81	−0.88	−0.64
Acetate (6)	1.91	—	+0.68	+0.54	+0.55	—	—
O-acetyl-glycoprotein (33)	2.07	—	+0.81	+0.83	+0.75	+0.80	—
Choline (31)	3.18	—	+0.61	+0.89	+0.61	+0.67	+0.55
Phosphatidylcholine (32)	3.21	—	−0.59	−0.70	−0.79	−0.84	−0.85
Creatine (13)	3.02	—	+0.54	+0.76	+0.72	+0.82	+0.77
Lipoprotein (25)	0.84	—	—	−0.72	−0.61	−0.75	−0.76
Unknown	2.34	—	+0.50	—	+0.50	+0.63	+0.87

*Numbers in parentheses refer to metabolites shown in Fig. 1, Fig. 2, and Fig. S2.

mice. Separation between infected and preinfected mice was enhanced at later time points, as suggested by higher Q^2 values. At later time points, the levels of the metabolites identified at day 7 were further differentiated from the preinfection group and additional metabolites, such as 2-oxoisovalerate, 3-carboxy-2-methyl-3-oxopropanamine, D-3-hydroxybutyrate, and lactate, were significantly elevated in the urine of infected mice.

Characterization of Sequential Plasma Metabolic Changes Associated with *T. brucei brucei* Infection. O-PLS-DA indicated systematic differentiation of plasma obtained from the *T. brucei brucei*-infected and preinfected mice. A selected O-PLS-DA coefficient plot, comparing plasma from a control mouse and that from day 14 postinfection, is shown in Fig. S2*B*). The quality of models indicated by the R^2 and Q^2 was good for all time points postinfection and are listed together with the significance of metabolites contributing to the differentiation between the plasma obtained from the post-infected and preinfected mice in Table 2. Plasma samples obtained as early as 1 day postinfection could be discriminated from those of preinfected mice and were typified by increased concentrations of lactate, oxaloacetate, and glucose, and decreased concentrations of glutamine, and lysine. Increasingly significant differentiation between preinfection and postinfection samples was achieved at later time points, which is consistent with the urinary metabolite data. Additional metabolites accounted for the separation between the *T. brucei brucei*-infected and preinfected mice at day 7 post-infection and later on, including elevated levels of acetate, *O*-acetylglycoprotein fragment signals, choline, and creatine, depleted levels of phosphatidylcholine, lipoproteins, and a range of amino acids, including isoleucine, valine, and leucine (Table 2). In addition, a plasma resonance at δ 2.34 from an unidentified metabolite was also increased in infected mice. The pattern of infection-induced metabolite perturbations was broadly consistent across all of the time points from day 7, with exception of glutamine and acetate, which showed a high degree of interanimal variation in levels after day 14. The concentration of glucose, increased at day 1 postinfection returning to preinfection levels at day 7 postinfection. However, a significant decrease in plasma glucose concentrations occurred at days 28 and 33 postinfection.

The decreased concentration of valine in the blood plasma, and increased urinary excretion of ketone bodies were suggestive of increased ketogenesis in the infected mice and therefore the valine to alanine ratio was measured by integration of the valine and alanine resonances in the plasma spectra. A significant and enduring decrease in this ratio occurred from day 7 postinfection (Fig. S3).

Discussion

A range of systemic metabolic perturbations in response to a *T. brucei brucei* infection in the mouse was observed with the earliest detection limit being day 1 postinfection in plasma and day 7 postinfection in urine. Several of the observed metabolic changes depended on time, and therefore stage of infection. The response to infection became stronger, and the degree of interanimal variability greater in the urine and plasma profiles as the time course evolved. Previous research has shown that *T. brucei brucei* parasites of the GVR35 strain were established in the brains of mice and rats at days 21 and 13 postinfection, respectively (4, 20). Our satellite experiment (*SI Text*) revealed that *T. brucei brucei* had already crossed the blood–brain barrier within 7 days of infection, therefore considerably earlier than we had anticipated. This early establishment of parasites in the brain may reflect an increase in the virulence of the *T. brucei brucei* strain used, which might be explained by prolonged passages in the laboratory (19). Such occurrences warrant further investigation with respect to interspecies differences in host-parasite behavior.

The current method of choice for diagnosis of first-stage HAT is based on microscopic detection of trypanosomes in blood and lymph node aspirate. Examination of cerebrospinal fluid is necessary in all patients to assess whether the parasites have penetrated into the brain (21). The obvious drawbacks of this method are that it is labor-intensive and invasive. In the present investigation, differentiation of metabolic profiles was achieved in mouse plasma already at day 1 postinfection onwards and in urine obtained from day 7 after infection. In addition, the PCA trajectory of ^{1}H NMR spectra of plasma and urine samples illustrated relocations in the metabolic space as well as more dispersed metabolic profiles between days 14 and 21 postinfection. This finding suggests increasing severity of disease and greater interanimal variation at later time points. Because the trypanosomes were already established in the CNS by day 7 postinfection, it seems difficult to identify a set of metabolic changes associated specifically with this event.

An elevated level of lactate was observed in both the urine and plasma obtained from mice after infection. This observation suggests an up-regulation of glycolysis in *T. brucei brucei*-infected mice, which is the likely result of parasites in the bloodstream. Previous research has shown that *T. brucei brucei* depends solely on glycolysis for its supply of ATP (22). In the current study, the relative concentration of glucose increased on the first day after infection, but then remained fairly constant until days 28 and 33 postinfection, when a marked reduction in glucose concentrations was observed. The observed initial rise in plasma glucose is consistent with previous research, which showed that *T. brucei* infection produced

a condition resembling type 2 diabetes characterized by increased concentrations of urinary ketogenic acids, together with decreased peripheral glucose utilization, which responded to insulin (23). This diabetes-like state was also present throughout the course of the disease, but was counteracted by the high rate of glucose utilization by *T. brucei* as an energy substrate. Indeed, severe hypoglycemia has been attributed to be the cause of death in trypanosomiasis (24, 25), and parenteral administration of glucose has been shown to delay, but not prevent death, suggesting the involvement of more than one pathogenic process (25). Moreover, mice chronically infected with *T. brucei gambiense* had significantly increased levels of pyruvate, and lactate, among other metabolites, pointing to an increased glycogen mobilization and increased catabolic activity (26), which is in line with our observations.

We noted the depletion of plasma amino acids, including glutamine, leucine, isoleucine, and valine in plasma samples obtained from *T. brucei brucei*-infected mice. Glutamine is a gluconeogenic amino acid and could provide a source for maintaining a normal level of glucose in infected animals. The depletion of other plasma amino acids may also reflect a compensatory mechanism for maintaining host energy homeostasis and ketogenesis. In addition, there was an associated increase in urinary concentrations of the keto acids, 3-methyl-2-oxovalerate and 2-oxoisovalerate. This association suggested that there was stimulation of ketogenesis in *T. brucei brucei*-infected mice because ketogenic amino acids are capable of producing keto acids via aminotransferases (26). A decreasing valine to alanine ratio in plasma samples from infected, but not control, animals was noted from day 7 postinfection persisting over the study duration, which concurs with the hypothesis of increased ketogenesis. Because alanine is a gluconeogenic amino acid, and valine (also isoleucine and leucine) is ketogenic, we suggest that the simple measurement of the plasma valine to alanine ratio from plasma NMR spectra may provide a useful window on the balance of ketogenesis and gluconeogenesis *in vivo*.

As the disease progressed, increased levels of D-3-hydroxybutyrate were noted in the urine of infected mice (Table 1). This observation suggested that at the later stage of the infection, animals were in a ketotic state and lipids were metabolized as an energy source. Reduced levels of lipids in plasma of infected mice were observed, consistent with the ketotic state of the animals (Table 2).

Hepatic extramedullary hemopoiesis was observed in all infected animals at 33 days postinfection (Fig. S1). Significantly increased serum levels of alanine aminotransferase and aspartate aminotransferase have been noted in infected animals (27). The reported increase in the levels of these enzymes is consistent with *T. brucei brucei*-induced liver damage. Interestingly, aspartate aminotransferases have also been cloned and expressed from *T. brucei brucei* (28). Another pathologic consequence of a trypanosome infection is renal damage, which has been found in the rat (29), and in the rabbit (30). In the present study, kidney pathology manifested as interstitial nephritis. In addition, *O*-acetylglycoprotein fragments were found in increased concentrations in the plasma of the infected mice, and may be reflective of tubular damage (Table 2).

Potent inflammatory responses of the host triggered by trypanosomes have been suggested as an underlying factor in the pathogenesis of this infection (31). The dominant inflammatory response presents as an increase in Ig levels and a range of cytokines, including IL-6, IL-10, and the proinflammatory cytokine tumor necrosis factor (TNF)-α have been found to be elevated in the meningo-encephalitic stage (32). In the current study, increased intensity of *O*-acetyl glycoprotein fragment resonance was observed in infected mice. Elevated *O*-acetyl glycoprotein fragment signals from acute phase reactive protein in rat blood plasma was considered to be associated with inflammatory conditions, such as cancer, certain liver diseases, and also during surgical trauma (33, 34).

It is known that parasitic protozoa have a membrane and a surface coat that has a different lipid and protein composition relative to the membrane of the host (35). Several reports on *T. brucei* have indicated that the parasites are capable of scavenging phospholipids from their host and rapidly incorporating these phospholipids into the membrane structure. In addition, bloodstream stage trypanosomes are able to take up low density lipoproteins from the host for robust growth (36, 37). The reduced concentrations of phosphatidylcholine and lipoproteins were accompanied by elevated levels of choline in the plasma of infected mice. This association most likely indicates a breakdown of choline-containing phospholipids by trypanosomes.

In the current study, reduced concentration of hippurate and increased concentrations of trimethylamine, and 4-hydroxyphenylacetic acid were observed in urine from infected mice. The reduced excretion of urinary hippurate was also observed in *S. mansoni*-infected mice and in *S. japonicum*-infected hamsters (14, 18). Therefore, it has been suggested that hippurate was associated with the disturbance of microbial activity. Trimethylamine is also derived from the intestinal bacterial degradation of choline (38) that is present in high level in the infected mice because of breakdown of choline-containing fatty acids. Evidence from the investigations of host-parasite interactions have suggested that the introduction of parasites into the mammalian system could disrupt normal mammalian-microbial behavior, thereby causing variation in metabolism. The major distinguishing consequences of a *T. brucei brucei* infection in the mouse were elevated levels of urinary 3-methyl-2-oxovalerate, 3-carboxy-2-methyl-3-oxopropanamine and 4-hydroxyphenyl acetic acid, when compared with a *Schistosoma* spp. infection in rodents. Additionally, for metabolic changes, which were in common; e.g., decreased excretion of hippurate, the dynamic progression of the infection differs (14, 18).

The role of rodent models in the investigation of HAT has been debated (39). The current consensus is that, although not perfect, mouse models can provide a useful means of investigating both the mechanism of pathogenesis and response to therapeutics. The metabonomic strategy presented here shows diagnostic potential for presence of infection and stage of disease. Ongoing studies investigating the transferability of the differentiating biomarkers, together with further animal studies exploring the specificity of the biofluid metabolite alteration in relation to other parasitic infections, should provide evidence of the utility of metabolic profiling in the mouse, as a model to deepen our understanding of HAT.

In conclusion, we have profiled the dynamic metabolic response of a *T. brucei brucei* infection in the mouse over the entire disease time course. We found systematic variations between *T. brucei brucei*-infected and the corresponding animals before infection in the metabolic profiles of plasma and urine using a NMR-based metabonomic strategy. The results obtained from both types of biofluids are consistent, underscoring evidence concerning the mechanisms of a trypanosome infection. The insights into biological response could provide vital information for targeted drug discovery and novel diagnostic tools. Moreover, we have demonstrated that the severity of the infection could be monitored using a PCA trajectory, and that infection-induced alteration could be detected as early as 1 day postinfection. Our investigation therefore demonstrates the usefulness of metabonomics as a tool for the investigation of host metabolic responses to pathogen invasion and for monitoring disease development and responses to control interventions.

Materials and Methods

Animal Handling and Sample Collection. The study protocol was approved by the institutional review boards of the Swiss Tropical Institute (Basel, Switzerland) and Imperial College (London, U.K.). The experiments were in compliance with cantonal and Swiss national regulations (permission no. 2081). For the main metabolic profiling experiment, a total of 24 female mice (NMRI strain), aged ≈3 weeks, weighing 20–24 g, were purchased from RCC (Füllinsdorf, Switzerland). Mice were housed in groups of 4 at the animal facilities of the Swiss Tropical Institute under environmentally controlled conditions (temperature, ≈22°C; rel-

ative humidity, ≈70%; day-night light cycle, 12–12 h) and acclimatized for 7 days. Mice had free access to water and standard rodent diet obtained from NAFAG (Gossau, Switzerland). Twelve mice were infected i.p. with ≈20,000 *T. brucei brucei* (GVR35 strain) each. The remaining 12 mice were left untreated, serving as controls.

Urine and blood plasma for ^{1}H NMR spectroscopic analysis were collected from each mouse 2 days preinfection and on days 1, 7, 14, 21, 28, and 33 postinfection. Blood samples were also collected for parasitemia testing from day 7 postinfection onwards. Animals were weighed at each time point, using a Mettler balance (model K7T; Greifensee, Switzerland). Collection of urine and blood plasma was carried out according to standardized procedures (14, 18) (*SI Text*).

Establishing the Time Frame at Which Trypanosomes Crossed the Blood–Brain Barrier. The experimental setup of this satellite study is provided in *SI Text* and results are presented in Table S1.

^{1}H NMR Spectroscopy. Urine samples were prepared by mixing 20 μl of urine with 30 μl of phosphate buffer (pH 7.4) containing 50% D_2O as a field frequency lock and 0.05% sodium 3-(tri-methylsilyl) propionate-2,2,3,3-d4 (TSP) as a chemical shift reference (δ 0.0). Plasma samples were prepared by adding 30 μl of saline containing 50% D_2O in an Eppendorf tube containing ≈20 μl of plasma. Samples were then transferred into 1.7-mm microNMR tubes. Standard 1D ^{1}H NMR spectra were recorded on a Bruker Avance 600 NMR spectrometer operating at 600.13 MHz (14). Additionally, water-suppressed Carr-Purcell-Meiboom-Gill (CPMG) (40) spectra were acquired for plasma, and metabolites were assigned from the literature (41) and from 2-dimensional (2D) NMR spectra including ^{1}H-^{1}H COSY, TOCSY, and ^{1}H J-resolved NMR spectra acquired for a selection of plasma sample using parameters described in previous studies (14).

Data Reduction and Pattern Recognition. Spectra were automatically corrected for phase and baseline distortion by using an in-house developed MATLAB script (Imperial College, London, U.K.). The blood plasma spectra were referenced to the anomeric proton of glucose resonance at δ5.223. The plasma spectra over the range δ 0.6–8.0 were digitized into 14,800 points by using a MATLAB script developed in-house (Imperial College, London, U.K.) (42). The region δ4.40–5.19 was removed to avoid the residual spectral effects of imperfect water suppression. Normalization to the sum of the spectrum was carried out on these data before pattern recognition analyses (42). Urine spectra were referenced to TSP at δ0.0 and digitized in the same way as plasma spectra. NMR regions δ4.50–4.90 and δ5.29–6.30 were removed. Normalization to the total sum of the spectrum was also carried out in the same way as for plasma spectra. In the first instance, PCA was performed on all data by using mean-centered data with the software SIMCA-P 10.00 (Umetrics, Umeå, Sweden). A further PCA model was constructed for the preinfection and days 1–14 inclusive postinfection samples to clarify the response observed at the early stage of infection. O-PLS-DA (13) of the NMR spectra was also carried out on the same data after scaling to unit variance in a MATLAB 7.0 environment with MATLAB script developed in-house (Imperial College, London, U.K.) (42). This procedure involved combining of orthogonal signal correction and partial least square-discriminant analysis as described by Trygg (13). It also incorporated back transformation of the coefficient plot with weight of the variable contributing to discrimination in the models and facilitating interpretation. The statistical total correlation spectroscopy (STOCSY) (43) method, based on the high correlation coefficient computed from signals from the same molecule, was also applied to aid metabolite assignment.

ACKNOWLEDGMENTS. We thank G. Riccio for help in the laboratory and Dr. O. Cloarec for providing in-house software. This study received financial support from the Swiss National Science Foundation (project PPOOB-102883). The authors also acknowledge Nestlé S.A. for provision of funds for Y.W.

1. Hotez PJ, *et al.* (2007) Control of neglected tropical diseases. *N Engl J Med* 357:1018–1027.
2. Fevre EM, Picozzi K, Jannin J, Welburn SC, Maudlin I (2006) Human African trypanosomiasis: Epidemiology and control. *Adv Parasitol* 61:167–221.
3. Barrett MP, *et al.* (2003) The trypanosomiases. *Lancet* 362:1469–1480.
4. Kennedy PGE (2004) Human African trypanosomiasis of the CNS: Current issues and challenges. *J Clin Invest* 113:496–504.
5. Stich A, Abel PM, Krishna S (2002) Human African trypanosomiasis. *BMJ* 325:203–206.
6. Barrett MP, Boykin DW, Brun R, Tidwell RR (2007) Human African trypanosomiasis: Pharmacological re-engagement with a neglected disease. *Br J Pharmacol* 152:1155–1171.
7. Wang CC (1995) Molecular mechanisms and therapeutic approaches to the treatment of African trypanosomiasis. *Annu Rev Pharmacol Toxicol* 35:93–127.
8. Magnus E, Vervoort T, Van Meirvenne N (1978) A card-agglutination test with stained trypanosomes (C.A.T.T.) for the serological diagnosis of *T. b. gambiense* trypanosomiasis. *Ann Soc Belg Med Trop* 58:169–176.
9. Hutchinson OC, Webb H, Picozzi K, Welburn S, Carrington M (2004) Candidate protein selection for diagnostic markers of African trypanosomiasis. *Trends Parasitol* 20:519–523.
10. Kennedy PGE (2006) Diagnostic and neuropathogenesis issues in human African trypanosomiasis. *Int J Parasitol* 36:505–512.
11. Agranoff D, Stich A, Abel P, Krishna S (2005) Proteomic fingerprinting for the diagnosis of human African trypanosomiasis. *Trends Parasitol* 21:154–157.
12. Papadopoulos MC, *et al.* (2004) A novel and accurate diagnostic test for human African trypanosomiasis. *Lancet* 363:1358–1363.
13. Trygg J (2002) O2-PLS for qualitative and quantitative analysis in multivariate calibration. *J Chemometr* 16:283–293.
14. Wang YL, *et al.* (2004) Metabonomic investigations in mice infected with *Schistosoma mansoni*: An approach for biomarker identification. *Proc Natl Acad Sci USA* 101:12676–12681.
15. Brindle JT, *et al.* (2002) Rapid and noninvasive diagnosis of the presence and severity of coronary heart disease using ^{1}H NMR-based metabonomics. *Nat Med* 8:1439–1444.
16. Solanky KS, *et al.* (2005) Biofluid ^{1}H NMR-based metabonomic techniques in nutrition research–metabolic effects of dietary isoflavones in humans. *J Nutr Biochem* 16:236–244.
17. Wang YL, *et al.* (2005) A metabonomic strategy for the detection of the metabolic effects of chamomile (*Matricaria recutita* L.) ingestion. *J Agri Food Chem* 53:191–196.
18. Wang YL, *et al.* (2006) System level metabolic effects of a *Schistosoma japonicum* infection in the Syrian hamster. *Mol Biochem Parasitol* 146:1–9.
19. Ebert D (1998) Experimental evolution of parasites. *Science* 282:1432–1435.
20. Darsaud A, *et al.* (2003) Clinical follow-up in the rat experimental model of African trypanosomiasis. *Exp Biol Med* 228:1355–1362.
21. Chappuis F, Loutan L, Simarro P, Lejon V, Buscher P (2005) Options for field diagnosis of human African trypanosomiasis. *Clin Microbiol Rev* 18:133–146.
22. Bakker BM, Michels PAM, Opperdoes FR, Westerhoff HV (1999) What controls glycolysis in bloodstream form *Trypanosoma brucei*? *J Biol Chem* 274:14551–14559.
23. Voorheis H (1969) The effect of *T. brucei* (S-42) on host carbohydrate metabolism: Liver production and peripheral tissue utilization of glucose. *Trans R Soc Trop Med Hyg* 63:122–123.
24. Hoppe J, Chapman C (1947) Role of glucose in acute parasitemic death of the rat infected with *Trypanosoma equiperdum*. *J Parasitol* 33:509–516.
25. Herbert WJ, Mucklow MG, Lennox B (1975) The cause of death in acute murine trypanosomiasis. *Trans R Soc Trop Med Hyg* 69:4.
26. Umar IA, Toh ZA, Igbalajobi FI, Gidado A, Buratai LB (2000) The role of vitamin C administration in alleviation of organ damage in rats infected with *Trypanosoma brucei*. *J Clin Biochem Nutr* 28:1–7.
27. Moon A, Williams J, Witherspoon C (1968) Serum biochemical changes in mice infected with *Trypanosoma rhodesiense* and *Trypanosoma duttoni*. *Exp Parasitol* 22:112–121.
28. Berger LC, Wilson J, Wood P, Berger BJ (2001) Methionine regeneration and aspartate aminotransferase in parasitic protozoa. *J Bacteriol* 183:4421–4434.
29. Biswas D, Choudhury A, Misra KK (2001) Histopathology of *Trypanosoma (Trypanozoon) evansi* infection in bandicoot rat. I. Visceral organs. *Exp Parasitol* 99:148–159.
30. Umar IA, Wuro-Chekke AU, Gidado A, Igbokwe IO (1999) Effects of combined parenteral vitamins C and E administration on the severity of anaemia, hepatic and renal damage in *Trypanosoma brucei brucei* infected rabbits. *Vet Parasitol* 85:43–47.
31. MacLean L, *et al.* (2004) Severity of human African trypanosomiasis in East Africa is associated with geographic location, parasite genotype, and host inflammatory cytokine response profile. *Infect Immun* 72:7040–7044.
32. Vincendeau P, Bouteille B (2006) Immunology and immunopathology of African trypanosomiasis. *Ann Braz Acad Sci* 78:645–665.
33. Grootveld M, *et al.* (1993) High-resolution proton NMR investigations of rat-blood plasma: Assignment of resonances for the molecularly mobile carbohydrate side-chains of acute-phase glycoproteins. *FEBS Lett* 322:266–276.
34. Afzali B, *et al.* (2003) Raised plasma total sialic acid levels are markers of cardiovascular disease in renal dialysis patients. *J Nephrol* 16:540–545.
35. Costa-Serrano A, Almeida IC, Freitas LH, Yoshida N, Schenkman S (2001) The mucin-like glycoprotein super-family of *Trypanosoma cruzi*: Structure and biological roles. *Mol Biochem Parasitol* 114:143–150.
36. Morita YS, Paul KS, Englund PT (2000) Specialized fatty acid synthesis in African trypanosomes: Myristate for CPI anchors. *Science* 288:140–143.
37. Samad A, Licht B, Stalmach ME, Mellors A (1988) Metabolism of phospholipids and lysophospholipids by trypanosoma-brucei. *Mol Biochem Parasitol* 29:159–169.
38. Seibel BA, Walsh PJ (2002) Trimethylamine oxide accumulation in marine animals: Relationship to acylglycerol storage. *J Exp Biol* 205:297–306.
39. Kennedy PGE (2007) Animal models of human African trypanosomiasis: Very useful or too far removed? *Trans R Soc Trop Med Hyg* 101:1061–1062.
40. Meiboom S, Gill D (1958) Modified spin-echo method for measuring nuclear relaxation times. *Rev Sci Instrum* 29:688–691.
41. Nicholson JK, Foxall PJD, Spraul M, Farrant RD, Lindon JC (1995) 750-MHz ^{1}H and ^{1}H-^{13}C NMR spectroscopy of human blood-plasma. *Anal Chem* 67:793–811.
42. Cloarec O, *et al.* (2005) Evaluation of the orthogonal projection on latent structure model limitations caused by chemical shift variability and improved visualization of biomarker changes in H-1 NMR spectroscopic metabonomic studies. *Anal Chem* 77:517–526.
43. Cloarec O, *et al.* (2005) Statistical total correlation spectroscopy: An exploratory approach for latent biomarker identification from metabolic ^{1}H NMR data sets. *Anal Chem* 77:1282–1289.